AGU PUBLICATIONS

Geophysical Research Letters

RESEARCH LETTER
10.1002/2017GL074098

Key Points:
- Comprehensive seamount databases provide new constraints on the volume of partial melt erupted from the asthenosphere
- On young seafloor, seamount volumes equate to a ~20 m thick layer, corresponding to extraction of 0.1% melt from 20 km of asthenosphere
- Greater seamount volumes on Cretaceous seafloor indicate greater melt extraction in the past and additional eruption on older seafloor

Correspondence to:
C. P. Conrad,
c.p.conrad@geo.uio.no

Citation:
Conrad, C. P., K. Selway, M. M. Hirschmann, M. D. Ballmer, and P. Wessel (2017), Constraints on volumes and patterns of asthenospheric melt from the space-time distribution of seamounts, *Geophys. Res. Lett.*, *44*, 7203–7210, doi:10.1002/2017GL074098.

Received 9 MAY 2017
Accepted 8 JUL 2017
Accepted article online 14 JUL 2017
Published online 25 JUL 2017

Constraints on volumes and patterns of asthenospheric melt from the space-time distribution of seamounts

Clinton P. Conrad[1], Kate Selway[2], Marc M. Hirschmann[3], Maxim D. Ballmer[4], and Paul Wessel[5]

[1]Centre for Earth Evolution and Dynamics, University of Oslo, Oslo, Norway, [2]Department of Earth and Planetary Sciences, Macquarie University, North Ryde, New South Wales, Australia, [3]Department of Earth Sciences, University of Minnesota, Minneapolis, Minnesota, USA, [4]Institute of Geophysics, ETH Zurich, Zurich, Switzerland, [5]Department of Geology and Geophysics, SOEST, University of Hawai'i at Mānoa, Honolulu, Hawaii, USA

Abstract Although partial melt in the asthenosphere is important geodynamically, geophysical constraints on its abundance remain ambiguous. We use a database of seamounts detected using satellite altimetry to constrain the temporal history of erupted asthenospheric melt. We find that intraplate volcanism on young seafloor (<60 Ma) equates to a ~20 m thick layer spread across the seafloor. If these seamounts tap partial melt within a ~20 km thick layer beneath the ridge flanks, they indicate extraction of an average melt fraction of ~0.1%. If they source thinner layers or more laterally restricted domains, larger melt fractions are required. Increased seamount volumes for older lithosphere suggest either more active ridge flank volcanism during the Cretaceous or additional recent melt eruption on older seafloor. Pacific basin age constraints suggest that both processes are important. Our results indicate that small volumes of partial melt may be prevalent in the upper asthenosphere across ocean basins.

Plain Language Summary Thousands of volcanic mountains known as "seamounts" lie beneath the world's oceans. These volcanoes are produced by the eruption of melted rock onto the Earth's surface, but it is unknown how much melted rock has been erupted onto the seafloor to produce the seamounts. We can now estimate this using new catalogs of seamounts that have been detected by satellites. We find that the world's seamounts, if spread out, would cover the seafloor with a rocky layer at least 18 m thick. We find that about half of this thickness is produced on newly created seafloor in the middle of the oceans and the other half accumulates after the seafloor ages to more than 60 Myr. These estimates provide constraints on how much melted rock must be present beneath the Earth's surface to feed these volcanoes. In particular, we find that the 20 km immediately beneath the plates should contain about 0.1% melt. This small amount of melt may be important for weakening the rocks beneath the tectonic plates, which may enable their movement.

1. Introduction

Seamounts are submarine volcanoes that erupt onto the seafloor, either on the flanks of mid-ocean ridges or on older seafloor, and remain there as the lithosphere below them subsides and accumulates sediments with age (Figure 1). This volcanism arises from reservoirs of fractional melt in the asthenosphere that can be detected geophysically and that impact bulk mechanical properties such as viscosity [e.g., *Holtzman*, 2016].

Despite the importance of asthenospheric melt, geophysical constraints remain ambiguous about its volume and distribution. Seismic data image a sharp velocity reduction (the "Gutenberg-discontinuity") at 45–70 km depth beneath some oceanic lithosphere ranging in age from <5 to >120 Ma [e.g., *Schmerr*, 2012]. More ubiquitous is the deeper "low-velocity zone" (LVZ) with a velocity reduction of ~3–5% at a depth of ~100–150 km [*Nettles and Dziewoński*, 2008]. While partial melt is commonly invoked as an explanation for both features [e.g., *Harmon et al.*, 2009; *Sakamaki et al.*, 2013; *Sato et al.*, 1989; *Schmerr*, 2012; *Yang et al.*, 2007], explanations involving anisotropy [*Beghein et al.*, 2014], hydrogen content [*Karato and Jung*, 1998], solid state mantle mineralogy [*Stixrude and Lithgow-Bertelloni*, 2005], solid state attenuation [*Goes et al.*, 2012], and subsolidus grain boundary sliding [*Gribb and Cooper*, 1998; *Olugboji et al.*, 2013] have also been proposed. Magnetotelluric data have imaged strong conductive anomalies at 20–150 km depth at the East Pacific Rise [*Evans et al.*, 2005; *Key et al.*, 2013] and at ~50 km depth below ~23 Myr old lithosphere on the Cocos Plate [*Naif et al.*, 2013] that seem best explained by partial melt. However, at greater depths and in older

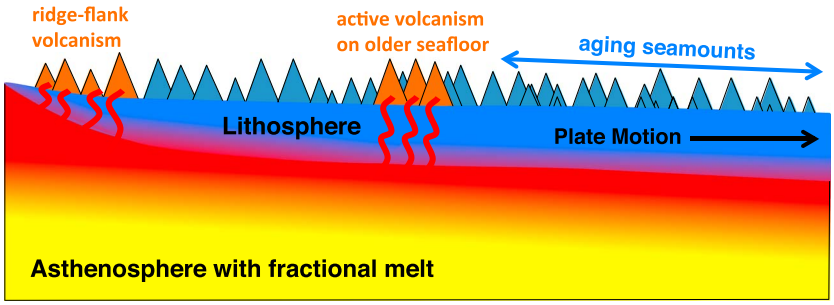

Figure 1. Seamounts erupt partial melts from the asthenosphere onto the seafloor (orange triangles), where they reside as the lithosphere ages (blue triangles). The distribution of seamounts on the seafloor thus constrains the distribution of eruptible asthenospheric melts.

oceanic lithosphere, analyses of existing magnetotelluric data have not unambiguously indicated the presence of partial melt [*Sarafian et al*., 2015; *Utada and Baba*, 2014]. Similarly, petrological data allow for the presence of a small degree of partial melt in the upper mantle but do not require it, depending on volatile concentrations [*Hirschmann*, 2010].

Recent analyses of satellite gravity observations have permitted identification of tens of thousands of seamounts [*Kim and Wessel*, 2011]. Such catalogs are likely incomplete for smaller seamounts due to detection difficulties for deep or thickly sedimented seafloor, but the threshold height for catalog completeness has recently approached 1 km due to improved techniques [*Wessel et al*., 2010] and may become further improved by radar altimetry [*Sandwell et al*., 2014]. We use seamounts catalogs to infer new constraints on the volume and distribution of asthenospheric melt available for eruption at some point in the seafloor's history. Such constraints could also help us to establish the timing of melt production and/or eruption, which may constrain the processes responsible for generating asthenospheric melt.

2. Seamount Volume Distributions

To estimate seamount volumes, we examine the seamount database of *Kim and Wessel* [2011], which contains location and volume information for 24,643 seamounts (Figure 2). Of these, about one third (8458) are taller than the completeness threshold of ~1 km. Smaller seamounts are more plentiful but are undercounted compared to expectations based on extrapolated size distributions, presumably due to obscuring by deep water and thick sediments [*Wessel et al*., 2010]. *Wessel* [1997] estimated unbiased measurement uncertainty of ~25% for seamount dimensions, although uncertainty in seamount volume is likely smaller because satellite gravity provides a more direct constraint. Because of sediment coverage, measured seamount volumes probably underestimate volumes of erupted melt, particularly for smaller seamounts.

Some seamounts lie within hot spot tracks associated with plumes originating from the deep mantle. Because our goal is to constrain melt volumes for ambient asthenosphere, we also estimate seamount volumes after removing these seamounts from the *Kim and Wessel* [2011] database. We drew envelopes around 22 hot spot tracks (Figure 2) interpreted by *Courtillot et al*. [2003] as fed by plumes arising from the deep lower mantle ("primary" plumes) or the base of the transition zone ("secondary" plumes). We use envelopes defined by *Maher et al*. [2015] for the African plate and by *Wessel and Kroenke* [2008] for the Pacific plate. On other plates, we drew tracks by hand from bathymetric maps using Google Earth. No seamounts lie within the Afar, Iceland, and Yellowstone hot spot envelopes (Figure 2), and two hot spot tracks on the Indian-Australian plate lie across ridge boundaries from their associated hot spots (the Chagos-Laccadive track associates with the Reunion Plume and the Ninety East track associates with Kerguelen). We compute seamount volume statistics both including and excluding the 1711 seamounts that lie within these defined hot spot tracks.

Using the seamount database, we compute the thickness of the volcanic layer that would be produced if all of the seamount volcanism within a given area of the seafloor were spread evenly across that area. This "seamount equivalent layer thickness" is directly related to the thickness of melt that must have been extracted from the asthenosphere at some point in the past to produce the observed seamount volcanism. For example, when spread across the entire seafloor, large non–hot spot seamounts would cover the seafloor

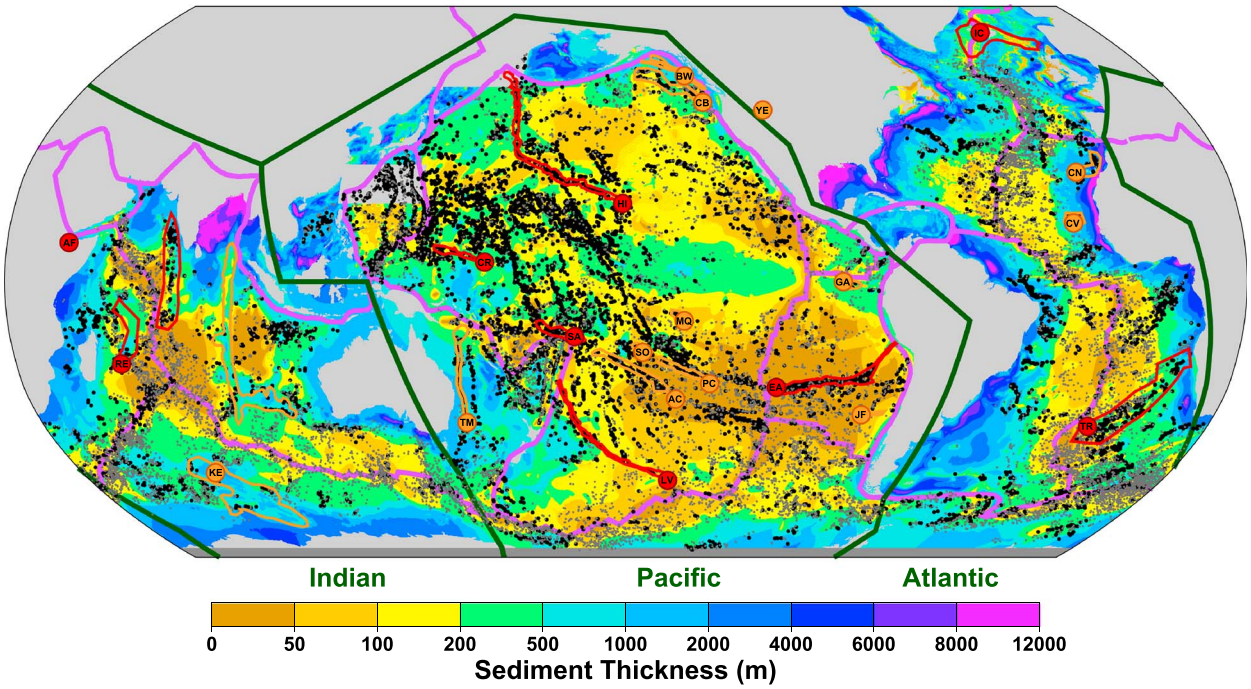

Figure 2. Seamount database of *Kim and Wessel* [2011], showing large (>1 km high, black dots) and small (<1 km, grey dots) seamounts atop the sediment thickness model of *Whittaker et al.* [2013] (background colors). Some seamounts lie within defined hot spot tracks that are grouped by *Courtillot et al.*'s [2003] distinction between those likely arising from the deep mantle (red envelopes; AF = Afar, CR = Carolina, EA = Easter, HI = Hawaii, IC = Iceland, LV = Louisville, RE = Reunion, SA = Samoa, and TR = Tristan) or the upper transition zone (orange envelopes: AC = Austral-Cook, BW = Bowie-Kodiak, CB = Cobb-Juan de Fuca, CN = Canary, CV = Cape Verde, GA = Galapagos, JF = Juan Fernandez, KE = Kerguelen, MQ = Marquesas, PC = Pitcairn, SO = Society-Tahiti, TM = Tasmanid, and YE = Yellowstone). Purple lines denote plate boundaries, and green lines denote boundaries between the Indian, Pacific, and Atlantic basins.

with a volcanic layer that is 17.9 m thick, while small seamounts would add an additional 6.2 m. The seamount equivalent thickness is not uniform across the seafloor: the layer thickness for large seamounts in the Pacific (24.2 m) is more than twice that of the Atlantic (12.0 m) and Indian (10.1 m) basins. In fact, large seamount equivalent thicknesses in the western Pacific can exceed 100 m (Figure 3a). Equivalent thicknesses for small seamounts are generally largest nearest to mid-ocean ridges (Figure 3b), where small seamounts are easier to detect.

To quantify the apparent relationship between seamount volume and seafloor age, we compute the seamount equivalent thickness within 10 million year seafloor age windows both globally and for each ocean basin (Figure 4). Globally, the seamount equivalent thickness near the ridges is about 11 m for both large and small seamounts. For large seamounts, this thickness increases with seafloor age (Figure 4a), either because of continued volcanic production as the seafloor ages or because this older seafloor experienced greater near-ridge volcanism in the past. Small seamounts, by contrast, exhibit diminishing volumes for older seafloor ages (Figure 4b), almost certainly because of decreasing detection capability moving away from the mid-ocean ridges. The exclusion of hot spot tracks makes almost no difference for small seamounts (Figure 4b) and generally decreases the seamount equivalent thickness by less than 20% for large seamounts (Figure 4a), with a slightly larger influence for older seafloor in the Pacific (e.g., associated with the Hawaiian, Samoan, and Caroline hot spot tracks).

3. Asthenospheric Melt Distribution Beneath Ridge Flanks

The seamount equivalent layer thickness for a given area of the seafloor constrains the total volume of melt that has been erupted onto that seafloor during its lifetime. Changes in this thickness across the seafloor help to constrain changes in the rate of volcanic emplacement with time. For example, the relatively flat curves for large seamounts on seafloor younger than ~60 Myr (Figure 4a) suggest that most of this volcanism erupted near the ridge; more widespread volcanism should produce an increase in seamount volumes with age,

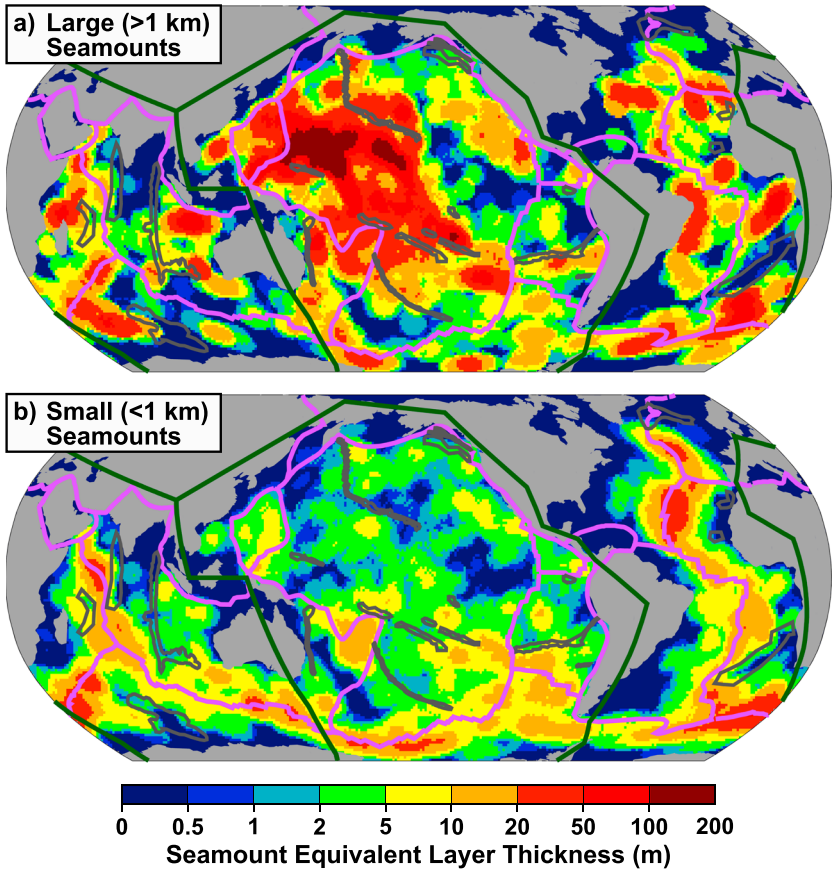

Figure 3. The volume of seamounts in the *Kim and Wessel* [2011] database, expressed as a layer thickness with a volume equivalent to that of all (a) large (heights >1 km) or (b) small (<1 km) seamounts within 500 km of every seafloor point. Seamounts associated with known plume tracks (dark grey outlines), are removed from the database before computing this "seamount equivalent layer thickness."

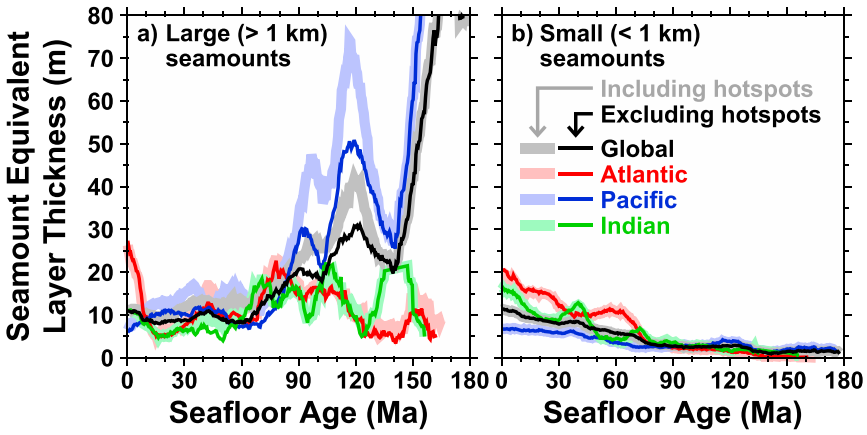

Figure 4. Average seamount equivalent layer thickness as a function of seafloor age, for (a) large seamounts (heights >1 km, data set thought to be complete) and (b) small seamounts (heights <1 km, trends likely represent observational bias) for each basin (red, blue, and green lines, for the Atlantic, Pacific, and Indian basins (as in Figure 2), and globally (black lines). Seafloor within hot spot tracks (Figure 2) is either included (light bands) or excluded (thin dark lines) from the thickness calculation.

which is not observed (except to some extent for the Pacific basin). In fact, both the Atlantic and Indian basins exhibit a decrease in large seamount volume away from the ridge for seafloor younger than ~20 Myr, which could reflect either sediment burial of large seamounts (Figure 2) or growing rates of near-ridge volcanism during this period. Globally, such temporal variations in near-ridge eruptions seem to average to a relatively flat curve at ~10 m thickness (Figure 4a), which implies relatively constant extraction of ~10 m of melt from the upper asthenosphere near the ridge to produce large seamounts during the past ~60 Myr.

Near the ridge, small seamounts contribute an additional ~10 m of melt to seafloor volcanism (Figure 4b), with the Atlantic and Indian basins contributing more than this value, and the Pacific basin less, as for large seamounts (Figure 4a). This similarity suggests that the processes responsible for ridge flank volcanism tend to produce both large and small seamounts in approximately equal volume proportions. Volumes of small seamounts diminish moving away from the ridge, but this is due to sampling difficulties for small seamounts and it is reasonable to assume that small seamounts contribute, on average, a volume equivalent to a ~10 m layer across seafloor younger than ~60 Myr. Together with large seamounts, this indicates that ~20 m of melt must be extracted from the asthenosphere within the first 10–20 Myr of plate creation. This extraction must be followed by relative quiescence until ~60 Myr.

If seamounts form due to opportunistic sampling of ambient melt beneath the ridge flank, then their volumes place a lower bound on the volume of that melt. For asthenosphere that is 30–200 km thick, as suggested by viscosity profiles inferred from postseismic relaxation studies [e.g., *Hu et al*., 2016], then ~20 m of melt is consistent with 0.01–0.07% melt distributed throughout the asthenosphere. If instead this melt ponds within a thin (~20 km) layer at the top of the asthenosphere [e.g., *Sakamaki et al*., 2013; *Schmerr*, 2012], then the melt fraction must be $>$0.1% because only a portion of the available melt might be erupted. Our estimate of $>$0.1% melt in the uppermost asthenosphere is within the bounds suggested by geophysical data. For instance, magnetotelluric constraints indicate laterally heterogeneous asthenospheric melt, with up to 1.0%–2.1% melt within the asthenosphere's uppermost ~25 km beneath ~23 Myr old Cocos Plate [*Naif et al*., 2013] and trace amounts of melt ($<$0.1%) in more poorly conductive oceanic regions [*Utada and Baba*, 2014]. Recent experimental data relating melt fractions to seismic velocities suggest that 0.5%–1% melt could account for the G-discontinuity velocity drop, with smaller melt fractions required for the LVZ [*Chantel et al*., 2016]. These very small inferred partial melt fractions are probably more volatile enriched and less SiO_2-poor ($<$40 wt %) [e.g., *Dasgupta et al*., 2013; *Hirschmann*, 2010] than intraplate seamount basalts [*Janney et al*., 2000; *Okumura and Hirano*, 2013]. However, during ascent from the asthenosphere, such melts likely react with overlying peridotite, becoming more silica enriched [*Keller et al*., 2017].

4. Asthenospheric Melt Distribution Beneath Older Seafloor

Seafloor older than ~60 Myr hosts approximately double the volume of large seamounts compared to younger seafloor for the Atlantic and Indian basins, and this ratio is even larger for the Pacific basin (Figure 4a). These greater volumes on older seafloor could result from faster near-ridge seamount production during the Cretaceous, when this seafloor was created. This explanation requires ridge flank seamount production to slow down along ridges in all ocean basins starting ~60 Myr ago. This seems unlikely, although flood basalt eruptions indicate that the Cretaceous was a period of intense igneous activity [*Coffin and Eldholm*, 1994; *Kerr et al*., 2000], which may have extended to non–hot spot seamount volcanism. However, such ridge flank volcanism should generally produce symmetrical patterns of seamount volumes across mid-ocean ridges. We cannot test this prediction for the Pacific because the former Farallon Plate has mostly subducted. In the Indian basin, regions of elevated seamount volcanism do not generally match across the ridge, except across the Southeast Indian Ridge (Figure 3a). In the Atlantic, excess seamount volumes off Brazil and New England have counterparts near Cameroon and Spain (Figure 3a) but most of these regions are associated with recent hot spot volcanism (e.g., Fernando, Great Meteor/New England, Cape Verde/Cameroon Line, and Madeiras/Canary hot spot pairs, respectively) that *Courtillot et al*. [2003] attribute to asthenospheric melts. This indicates that most ambient volcanism on older lithosphere, at least in the Indian and Atlantic basins, was generated after the seafloor had moved away from the ridge.

Thus, increased seamount volumes on lithosphere older than 60 Myr likely indicate a second period of seamount formation in all basins, but especially in the Pacific (Figure 4a). Indeed, several observations

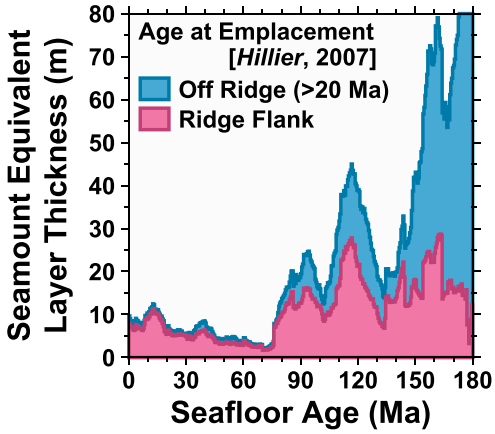

Figure 5. Average seamount equivalent layer thickness as a function of seafloor age, computed using the *Hillier* [2007] database for the Pacific Plate (excluding plume tracks), where hot spots emplaced on the ridge flank (seafloor <20 Myr old, red region) are distinguished from those emplaced off ridge (blue region).

indicate reheating of oceanic lithosphere after this age, including seafloor flattening [e.g., *Stein and Stein*, 1992; *Zhong et al*., 2007], geochemical observations [e.g., *Ballmer et al*., 2010], and disruption of oceanic seismic anisotropy [e.g., *van Hunen and Čadek*, 2009]. Furthermore, seismic observations of lithospheric thermal structure [e.g., *Ritzwoller et al*., 2004] indicate reheating older lithosphere, especially in the central and western Pacific [*Goes et al*., 2013], where seamount volumes are greatest (Figure 3a). This reheating, which could be generated by the onset of small-scale convection [e.g., *Huang et al*., 2003], may actively generate melt that is then volcanically sampled by seamount volcanism [*Ballmer et al*., 2009]. In this case, an additional 10 m average equivalent thickness of volcanism (Figure 4a) or more, if accompanied by additional undetectable small seamounts (Figure 4b), should represent the eruption of 0.05% melt or more from the upper 20 km of the asthenosphere. As before, seamount density exhibits significant lateral variability, presumably reflecting heterogeneous asthenospheric melt fraction that also might be larger if not all of the melt is erupted, or smaller if distributed over a greater thickness of the asthenosphere.

5. Melting History of the Pacific

The Pacific basin shows greater volumes of large seamounts on the Cretaceous seafloor than the Atlantic or Indian basins (Figure 4a), with equivalent layer thicknesses of 30–50 m. Again, we cannot determine whether this excess volcanism is due to greater ridge flank volcanism in the Cretaceous or more recent volcanism on older seafloor. Ages for some of these seamounts have been estimated by *Hillier* [2007], who used measurements of flexural wavelengths from crossing ship tracks to estimate elastic thicknesses, and thus lithospheric ages, for seamounts at the time of their emplacement. These ages allow ridge flank volcanism (emplaced on seafloor younger than ~20 Myr) to be distinguished from seamounts emplaced after the lithosphere moved away from the ridge. Since *Hillier*'s [2007] database is only for the Pacific Plate and is less complete than *Kim and Wessel*'s [2011] database, we use it to examine relative, rather than absolute, changes in seamount volcanism with age.

Ridge flank volcanism accounts for nearly all seamounts on Pacific Plate seafloor younger than ~60 Myr (Figure 5), consistent with our global analysis. Ridge flank seamounts on older seafloor exhibit approximately double the volume compared to younger seafloor (Figure 5). Beyond this doubling, most of the additional increase in seamount volumes on seafloor older than 60 Myr is due to seamounts that formed well away from the ridge flank. Relating these trends to the seamount volumes inferred from the more complete *Kim and Wessel* [2011] database (Figure 4a), we estimate that Pacific ridges accumulated about 20 m of seamount equivalent layer thickness during the Cretaceous from large seamounts. After 60 Ma, ridge flank volcanism decreased to ~10 m of large seamount equivalent layer thickness. These figures could be doubled if volumes for small seamounts change proportionally. *Conrad et al*. [2011] suggested that volcanism induced by shear-driven upwelling [*Conrad et al*., 2010] should have been faster on the Cretaceous Pacific Plate because of more rapid spreading at that time. The remaining 10–30 m of seamount equivalent thickness on Pacific seafloor older than 60 Myr was likely emplaced away from the ridges, possibly with the onset of convective instability after ~60 Myr. This volume is slightly larger than the extra ~10 m of large seamount thickness that we infer were added to the Indian and Atlantic lithosphere after it reached ~60 Myr (Figure 4a). The contribution of off-ridge seamount volcanism grows significantly (by >50 m) after ~150 Myr (Figure 5), which suggests continued, or even accelerated, seamount emplacement as the Pacific plate ages beyond 150 Myr (although Jurassic seafloor is undoubtedly anomalous).

6. Discussion and Conclusions

We have placed constraints on asthenospheric melt associated with two episodes of volcanism. The first occurs along the ridge flank (lithosphere younger than ~20 Myr) and produces seamounts equivalent to a ~20 m layer of volcanism along all ridges, and approximately double this figure in the Cretaceous Pacific Basin. The second episode emplaces at least another ~10 m equivalent of seamount volcanism onto the seafloor once the lithosphere ages to ~60 Myr. The timing of this additional volcanism is similar for all basins and is consistent with other observations of thermal alteration of the lithosphere starting after ~60 Myr. The spatial distribution of this additional volcanism is laterally variable, however, with some regions of the seafloor exhibiting significantly more seamount volcanism than others (Figure 3a) and the Pacific basin showing approximately double the volcanism of the other basins (Figure 4a).

By relating seamount volumes to asthenospheric melt fraction, we estimate that on average, ~20 m of melt is removed from the upper asthenosphere following lithosphere formation, and another 10 m or more after the lithosphere reaches 60 Ma. In both cases, this melt is laterally heterogeneous and could be sampled from an ambient asthenosphere reservoir or one dynamically generated by active mantle upwelling. However, these seamount volumes correspond to average extraction of ~0.1% partial melt from the upper 20 km of near-ridge asthenosphere (or other equivalent melt proportion and thickness products). How this melt fraction relates to the volume of melt currently present in the upper asthenosphere, which may be laterally heterogeneous, depends on how efficiently seamounts remove asthenospheric melt, which is unknown.

Our work sheds light on some of the ambiguities inherent to inferring melt from geophysical data. Even if the accumulated melt is effectively drained by seamount volcanism, a small volume of melt is thought to either accumulate at the lithosphere-asthenosphere boundary [*Sakamaki et al*., 2013] or remain retained within the asthenosphere due to a combination of surface tension forces and low permeability [*Hirschmann*, 2010; *Holtzman*, 2016]. Melt fractions of ~0.1% should still reduce seismic velocities by ~0.5% [*Chantel et al*., 2016] and, particularly if volatile rich, produce an observable conductivity anomaly [*Sifre et al*., 2014] and reduce peridotite viscosity by an order of magnitude or more [*Holtzman*, 2016]. Evidence for similar volumes of erupted melt within seamount catalogs suggests that partial melt should be considered when interpreting asthenospheric geophysical anomalies across oceanic plates.

Acknowledgments
This work was partly supported by the Research Council of Norway Centres of Excellence project 223272 and the Australian Research Council grant FT150100541. We used data from the references and *Kim and Wessel* [2011] seamount data available at http://www.soest.hawaii.edu/PT/SMTS/main.html.

References

Ballmer, M. D., G. Ito, J. van Hunen, and P. J. Tackley (2010), Small-scale sublithospheric convection reconciles geochemistry and geochronology of 'Superplume' volcanism in the western and south Pacific, *Earth Planet. Sci. Lett.*, *290*(1–2), 224–232, doi:10.1016/j.epsl.2009.12.025.

Ballmer, M. D., J. van Hunen, G. Ito, T. A. Bianco, and P. J. Tackley (2009), Intraplate volcanism with complex age-distance patterns: A case for small-scale sublithospheric convection, *Geochem. Geophys. Geosyst.*, *10*, Q06015, doi:10.1029/2009GC002386.

Beghein, C., K. Yuan, N. Schmerr, and Z. Xing (2014), Changes in seismic anisotropy shed light on the nature of the Gutenberg discontinuity, *Science*, *343*(6176), 1237–1240, doi:10.1126/science.1246724.

Chantel, J., G. Manthilake, D. Andrault, D. Novella, T. Yu, and Y. Wang (2016), Experimental evidence supports mantle partial melting in the asthenosphere, *Sci. Adv.*, *2*(5), doi:10.1126/sciadv.1600246.

Coffin, M. F., and O. Eldholm (1994), Large igneous provinces: Crustal structure, dimensions, and external consequences, *Rev. Geophys.*, *32*(1), 1–36, doi:10.1029/93RG02508.

Conrad, C. P., B. J. Wu, E. I. Smith, T. A. Bianco, and A. Tibbetts (2010), Shear-driven upwelling induced by lateral viscosity variations and asthenospheric shear: A mechanism for intraplate volcanism, *Phys. Earth Planet. Inter.*, *178*(3–4), 162–175, doi:10.1016/j.pepi.2009.10.001.

Conrad, C. P., T. A. Bianco, E. I. Smith, and P. Wessel (2011), Patterns of intraplate volcanism controlled by asthenospheric shear, *Nat. Geosci.*, *4*(5), 317–321, doi:10.1038/ngeo1111.

Courtillot, V., A. Davaille, J. Besse, and J. Stock (2003), Three distinct types of hotspots in the Earth's mantle, *Earth Planet. Sci. Lett.*, *205*(3–4), 295–308, doi:10.1016/S0012-821X(02)01048-8.

Dasgupta, R., A. Mallik, K. Tsuno, A. C. Withers, G. Hirth, and M. M. Hirschmann (2013), Carbon-dioxide-rich silicate melt in the Earth/'s upper mantle, *Nature*, *493*(7431), 211–215, doi:10.1038/nature11731.

Evans, R. L., G. Hirth, K. Baba, D. Forsyth, A. Chave, and R. Mackie (2005), Geophysical evidence from the MELT area for compositional controls on oceanic plates, *Nature*, *437*(7056), 249–252, doi:10.1038/nature04014.

Goes, S., J. Armitage, N. Harmon, H. Smith, and R. Huismans (2012), Low seismic velocities below mid-ocean ridges: Attenuation versus melt retention, *J. Geophys. Res.*, *117*, B12403, doi:10.1029/2012JB009637.

Goes, S., C. M. Eakin, and J. Ritsema (2013), Lithospheric cooling trends and deviations in oceanic PP-P and SS-S differential traveltimes, *J. Geophys. Res. Solid Earth*, *118*, 996–1007, doi:10.1002/jgrb.50092.

Gribb, T. T., and R. F. Cooper (1998), Low-frequency shear attenuation in polycrystalline olivine: Grain boundary diffusion and the physical significance of the Andrade model for viscoelastic rheology, *J. Geophys. Res.*, *103*(B11), 27,267–27,279, doi:10.1029/98JB02786.

Harmon, N., D. W. Forsyth, and D. S. Weeraratne (2009), Thickening of young Pacific lithosphere from high-resolution Rayleigh wave tomography: A test of the conductive cooling model, *Earth Planet. Sci. Lett.*, *278*(1–2), 96–106, doi:10.1016/j.epsl.2008.11.025.

Hillier, J. K. (2007), Pacific seamount volcanism in space and time, *Geophys. J. Int.*, *168*(2), 877–889, doi:10.1111/j.1365-246X.2006.03250.x.

Hirschmann, M. M. (2010), Partial melt in the oceanic low velocity zone, *Phys. Earth Planet. Inter.*, *179*(1–2), 60–71, doi:10.1016/j.pepi.2009.12.003.
Holtzman, B. K. (2016), Questions on the existence, persistence, and mechanical effects of a very small melt fraction in the asthenosphere, *Geochem. Geophys. Geosyst.*, *17*, 470–484, doi:10.1002/2015GC006102.
Hu, Y., R. Bürgmann, P. Banerjee, L. Feng, E. M. Hill, T. Ito, T. Tabei, and K. Wang (2016), Asthenosphere rheology inferred from observations of the 2012 Indian Ocean earthquake, *Nature*, *538*(7625), 368–372, doi:10.1038/nature19787.
Huang, J. S., S. J. Zhong, and J. van Hunen (2003), Controls on sublithospheric small-scale convection, *J. Geophys. Res.*, *108*(B8), 2405, doi:10.1029/2003JB002456.
Janney, P. E., J. D. Macdougall, J. H. Natland, and M. A. Lynch (2000), Geochemical evidence from the Pukapuka volcanic ridge system for a shallow enriched mantle domain beneath the South Pacific Superswell, *Earth Planet. Sci. Lett.*, *181*(1–2), 47–60, doi:10.1016/S0012-821X(00)00181-3.
Karato, S.-I., and H. Jung (1998), Water, partial melting and the origin of the seismic low velocity and high attenuation zone in the upper mantle, *Earth Planet. Sci. Lett.*, *157*(3–4), 193–207, doi:10.1016/S0012-821X(98)00034-X.
Keller, T., R. F. Katz, and M. M. Hirschmann (2017), Volatiles beneath mid-ocean ridges: Deep melting, channelised transport, focusing, and metasomatism, *Earth Planet. Sci. Lett.*, *464*, 55–68, doi:10.1016/j.epsl.2017.02.006.
Kerr, A. C., R. V. White, and A. D. Saunders (2000), LIP reading: Recognizing oceanic plateaux in the geological record, *J. Petrol.*, *41*(7), 1041–1056, doi:10.1093/petrology/41.7.1041.
Key, K., S. Constable, L. Liu, and A. Pommier (2013), Electrical image of passive mantle upwelling beneath the northern East Pacific rise, *Nature*, *495*(7442), 499–502, doi:10.1038/nature11932.
Kim, S.-S., and P. Wessel (2011), New global seamount census from altimetry-derived gravity data, *Geophys. J. Int.*, *186*(2), 615–631, doi:10.1111/j.1365-246X.2011.05076.x.
Maher, S. M., P. Wessel, R. D. Müller, S. E. Williams, and Y. Harada (2015), Absolute plate motion of Africa around Hawaii-Emperor bend time, *Geophys. J. Int.*, *201*(3), 1743–1764, doi:10.1093/gji/ggv104.
Naif, S., K. Key, S. Constable, and R. L. Evans (2013), Melt-rich channel observed at the lithosphere-asthenosphere boundary, *Nature*, *495*(7441), 356–359, doi:10.1038/nature11939.
Nettles, M., and A. M. Dziewoński (2008), Radially anisotropic shear velocity structure of the upper mantle globally and beneath North America, *J. Geophys. Res.*, *113*, B02303, doi:10.1029/2006JB004819.
Okumura, S., and N. Hirano (2013), Carbon dioxide emission to Earth's surface by deep-sea volcanism, *Geology*, *41*(11), 1167–1170, doi:10.1130/g34620.1.
Olugboji, T. M., S. Karato, and J. Park (2013), Structures of the oceanic lithosphere-asthenosphere boundary: Mineral-physics modeling and seismological signatures, *Geochem. Geophys. Geosyst.*, *14*, 880–901, doi:10.1002/ggge.20086.
Ritzwoller, M. H., N. M. Shapiro, and S. J. Zhong (2004), Cooling history of the Pacific lithosphere, *Earth Planet. Sci. Lett.*, *226*(1–2), 69–84, doi:10.1016/j.epsl.2004.07.032.
Sakamaki, T., A. Suzuki, E. Ohtani, H. Terasaki, S. Urakawa, Y. Katayama, K.-i. Funakoshi, Y. Wang, J. W. Hernlund, and M. D. Ballmer (2013), Ponded melt at the boundary between the lithosphere and asthenosphere, *Nat. Geosci.*, *6*(12), 1041–1044, doi:10.1038/ngeo1982.
Sandwell, D. T., R. D. Müller, W. H. F. Smith, E. Garcia, and R. Francis (2014), New global marine gravity model from CryoSat-2 and Jason-1 reveals buried tectonic structure, *Science*, *346*(6205), 65–67, doi:10.1126/science.1258213.
Sarafian, E., R. L. Evans, J. A. Collins, J. Elsenbeck, G. A. Gaetani, J. B. Gaherty, G. Hirth, and D. Lizarralde (2015), The electrical structure of the central Pacific upper mantle constrained by the NoMelt experiment, *Geochem. Geophys. Geosyst.*, *16*, 1115–1132, doi:10.1002/2014GC005709.
Sato, H., I. S. Sacks, and T. Murase (1989), The use of laboratory velocity data for estimating temperature and partial melt fraction in the low-velocity zone: Comparison with heat flow and electrical conductivity studies, *J. Geophys. Res.*, *94*(B5), 5689–5704, doi:10.1029/JB094iB05p05689.
Schmerr, N. (2012), The Gutenberg discontinuity: Melt at the lithosphere-asthenosphere boundary, *Science*, *335*(6075), 1480–1483, doi:10.1126/science.1215433.
Sifre, D., E. Gardes, M. Massuyeau, L. Hashim, S. Hier-Majumder, and F. Gaillard (2014), Electrical conductivity during incipient melting in the oceanic low-velocity zone, *Nature*, *509*(7498), 81–85, doi:10.1038/nature13245.
Stein, C. A., and S. Stein (1992), A model for the global variation in oceanic depth and heat flow with lithospheric age, *Nature*, *359*(6391), 123–129.
Stixrude, L., and C. Lithgow-Bertelloni (2005), Mineralogy and elasticity of the oceanic upper mantle: Origin of the low-velocity zone, *J. Geophys. Res.*, *110*, B03204, doi:10.1029/2004JB002965.
Utada, H., and K. Baba (2014), Estimating the electrical conductivity of the melt phase of a partially molten asthenosphere from seafloor magnetotelluric sounding data, *Phys. Earth Planet. Inter.*, *227*, 41–47, doi:10.1016/j.pepi.2013.12.004.
van Hunen, J., and O. Čadek (2009), Reduced oceanic seismic anisotropy by small-scale convection, *Earth Planet. Sci. Lett.*, *284*(3–4), 622–629, doi:10.1016/j.epsl.2009.05.034.
Wessel, P. (1997), Sizes and ages of seamounts using remote sensing: Implications for intraplate volcanism, *Science*, *277*(5327), 802–805, doi:10.1126/science.277.5327.802.
Wessel, P., and L. W. Kroenke (2008), Pacific absolute plate motion since 145 Ma: An assessment of the fixed hot spot hypothesis, *J. Geophys. Res.*, *113*, B06101, doi:10.1029/2007JB005499.
Wessel, P., D. T. Sandwell, and S.-S. Kim (2010), The global seamount census, *Oceanography*, *23*(1), 24–33, doi:10.5670/oceanog.2010.60.
Whittaker, J. M., A. Goncharov, S. E. Williams, R. D. Müller, and G. Leitchenkov (2013), Global sediment thickness data set updated for the Australian-Antarctic Southern Ocean, *Geochem. Geophys. Geosyst.*, *14*, 3297–3305, doi:10.1002/ggge.20181.
Yang, Y., D. W. Forsyth, and D. S. Weeraratne (2007), Seismic attenuation near the East Pacific rise and the origin of the low-velocity zone, *Earth Planet. Sci. Lett.*, *258*(1–2), 260–268, doi:10.1016/j.epsl.2007.03.040.
Zhong, S. J., M. Ritzwoller, N. Shapiro, W. Landuyt, J. S. Huang, and P. Wessel (2007), Bathymetry of the Pacific plate and its implications for thermal evolution of lithosphere and mantle dynamics, *J. Geophys. Res.*, *112*, B06412, doi:10.1029/2006JB004628.